

# Design, Synthesis, and Herbicidal Activity of Substituted 3-(Pyridin-2-yl)Phenylamino Derivatives

Zhongyin Chen, Hui Cai, Xiao Zhang, Meng Zhang, Ge-Fei Hao, Zhichao Jin, Shichao Ren,\* and Yonggui Robin Chi\*



Cite This: <https://doi.org/10.1021/acs.jafc.3c06144>



Read Online

ACCESS |

Metrics & More

Article Recommendations

Supporting Information

**ABSTRACT:** To discover protoporphyrinogen oxidase (PPO) inhibitors with robust herbicidal activity and crop safety, three types of substituted 3-(pyridin-2-yl)phenylamino derivatives bearing amide, urea, or thiourea as side chain were designed via structure splicing strategy. Postemergence herbicidal activity assessment of 33 newly prepared compounds revealed that many of our compounds such as **6a**, **7b**, and **8d** exhibited superior herbicidal activities against broadleaf and monocotyledon weeds to commercial acifluorfen. In particular, compound **8d** exhibited excellent herbicidal activities and high crop safety at a dosage range of 37.5–150 g ai/ha. PPO inhibitory studies supported our compounds as typical PPO inhibitors. Molecular docking studies revealed that compound **8d** provided effective interactions with *Nicotiana tabacum* PPO (NtPPO) via diverse interaction models, such as  $\pi$ – $\pi$  stacking and hydrogen bonds. Molecular dynamics (MD) simulation studies and degradation studies were also conducted to gain insight into the inhibitory mechanism. Our study indicates that compound **8d** may be a candidate molecule for the development of novel herbicides.

**KEYWORDS:** structural splicing, protoporphyrinogen oxidase, herbicidal activity, substituted 3-(pyridin-2-yl)phenylamino derivatives

## INTRODUCTION

Food shortage has become a significant global issue as the global population is expected to reach 9 billion by 2050, with an estimated requirement of about a 60% increase in food production to meet the surging demand.<sup>1</sup> However, the growth of weeds has become a serious threat to agricultural productivity. Indeed, approximately 34% of crop yields are lost due to weeds per year.<sup>2</sup> Weed control poses a critical challenge in agricultural production, and the utilization of herbicides has played a significant role in ensuring food production.<sup>3,4</sup> However, the long-term and extensive use of conventional herbicides such as acetolactate synthase inhibitors, acetyl-CoA carboxylase inhibitors, glyphosate, among others has raised concerns such as environmental pollution and the development of weed resistance.<sup>5–7</sup>

Among the developed herbicides, protoporphyrinogen oxidase inhibitors attract substantial attention due to their favorable environmental safety, low toxicity, low application dosage, and broad spectrum of weed control.<sup>8</sup> For example, several structures such as diphenyl ethers, pyrimidindiones, phenylpyrazoles, pyridazinones, and *N*-phenyl cyclic amides have been widely and deeply explored for PPO-inhibiting herbicides development.<sup>9–11</sup> Protoporphyrinogen oxidase (PPO) promotes the conversion of protoporphyrin IX to protoporphyrin IX in the presence of external oxygen. PPO inhibitors could effectively occupy the active cavity of the PPO enzyme and, therefore, significantly reduce its catalytic activity. Such inhibition subsequently hinders the biosynthesis of chlorophyll and hemoglobin and may even result in the generation of singlet oxygen to cause yellowing, wilting, desiccation of leaves, and eventually plant demise. Therefore,

PPO serves as a crucial target enzyme for the development of novel herbicides.<sup>12–14</sup> Despite a lot of attention has been devoted to the development of PPO inhibitors and a large number of PPO-inhibiting herbicides have been applied in agriculture production, the design and synthesis of structurally novel PPO-inhibiting herbicides against weed resistance with a broad spectrum of weed control and crop safety is still highly demanded.

Diphenyl ether motifs are one of the core structures in PPO inhibitors.<sup>15,16</sup> It is worth noting that based on the structural splicing strategy and the structure–activity relationship analysis of diphenyl ethers and pyrimidines, scientists have designed and synthesized a biphenyl compound with weak herbicidal activity. Subsequent work revealed that replacing the 2-Cl-4-CF<sub>3</sub>-phenyl moiety of the biphenyl compounds with 3-Cl-5-CF<sub>3</sub>-pyridine remarkably enhanced their herbicidal activity. This breakthrough has inspired the development of innovative PPO-inhibiting herbicides that bear a phenyl-pyridine skeleton (Figure 1A).<sup>17</sup>

On the other hand, halogen-substituted phenyl rings play a crucial role in the biological activity of agrochemicals.<sup>18</sup> Especially, the introduction of fluorine atoms into the phenyl ring is beneficial for enhancing the compounds' lipophilicity and increasing interactions between the active molecules and

**Received:** August 30, 2023

**Revised:** January 12, 2024

**Accepted:** January 12, 2024

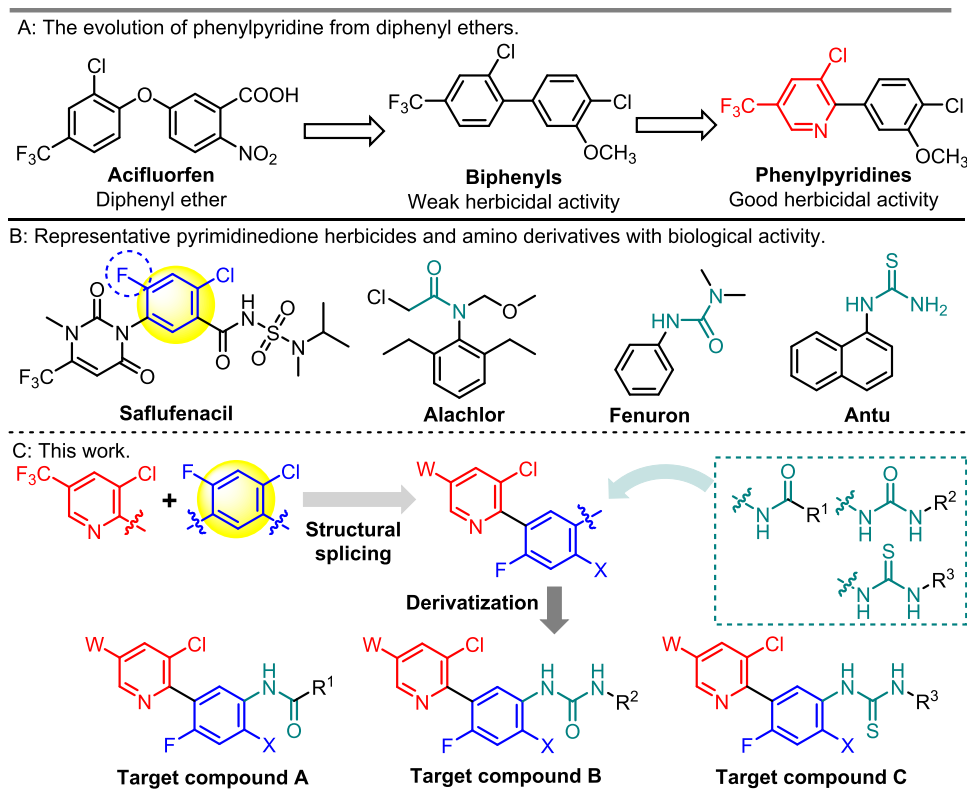


Figure 1. Design strategy of target compounds.

targets.<sup>19</sup> For example, saflufenacil and tiafenacil, developed by BASF and FarmHannong Co., Ltd., respectively, are PPO inhibitors with a broad-spectrum and highly effective herbicidal activity (Figure 1B). All of these herbicide molecules contain F and Cl atom-substituted phenyl rings.<sup>20</sup>

Due to our continuous interest in developing structurally novel molecules with agricultural activities,<sup>21–23</sup> we aimed to develop a novel fluorine-containing phenylpyridine scaffold with herbicidal activities by linking the trifluoromethylpyridine fragment with the halogen-substituted phenyl moiety of saflufenacil under the direction of the structural splicing strategy. Meanwhile, due to the wide range of biological activities of *N*-substituted amino derivatives (Figure 1B),<sup>24–26</sup> a side chain such as amide, urea, and thiourea would be installed on the phenylpyridine skeleton to modify the herbicidal activity. With this hypothesis in mind, three types of substituted 3-(pyridin-2-yl) phenylamino derivatives were designed and synthesized (Figure 1B). The postemergence herbicidal activity assessment of our compounds was conducted to evaluate their herbicidal activities. The results suggested that many of our compounds such as **6a**, **7b**, and **8d** exhibited superior herbicidal activities to commercial acifluorfen. In addition, computer-assisted techniques such as molecular docking studies, molecular dynamic (MD) simulation studies, and degradation studies were conducted to gain insight into the inhibitory mechanism. The excellent herbicidal activities (against broadleaf and monocotyledon weeds) and the high crop safety demonstrated compound **8d** as a potential candidate molecule for the development of novel herbicides.

## MATERIALS AND METHODS

**Chemicals and Instruments.** Chemical materials obtained from Bide or Aladdin were used as received. Proton nuclear magnetic

resonance (<sup>1</sup>H NMR) spectra were recorded on a Bruker (AVANCE III HD 400 MHz) spectrometer. Liquid chromatography–mass spectrometry (LC-MS) data were obtained using a 4000 Q TRAP instrument (AB Sciex). The melting point (m.p.) of the title compounds was determined when left untouched on an XT-4-MP apparatus from Beijing Tech. Instrument Co. (Beijing, China). The reaction process was monitored using Agilent 7890B-5977B gas chromatography–mass spectrometry (GC-MS).

**Synthesis of Compounds 6a–8j (Scheme 1).** *General Synthetic Procedure for 3a–3c.* Compound **1a** (2.38 g, 10 mmol), compound **2a** (1.92 g, 11 mmol), sodium carbonate (3.18 g, 30 mmol), and bis triphenylphosphine palladium(II) chloride (140.38 mg, 0.2 mmol) in dimethoxyethane (20 mL) and water (20 mL) were placed in a round-bottom flask and stirred at 60 °C. After the completion of the reaction was monitored by GC-MS, the temperature was lowered to room temperature, and the reaction system was filtered to remove the remaining solid sodium carbonate. The reaction mixture was extracted with ethyl acetate and saturated salt solution, retaining the organic layer. The solvent was evaporated, and the resulting mixture was subjected to column chromatography to isolate compound **3a**. Compounds **3b** and **3c** were prepared using the same method.<sup>27</sup> The <sup>1</sup>H NMR characterization data for compounds **3a–3c** are provided in the Supporting Information.

*General Synthetic Procedure for 4a–4c.* Compound **3a** (3.10 g, 10 mmol) was dissolved in concentrated sulfuric acid (98%) within an ice bath, maintaining a temperature range of 0–5 °C. Gradually, nitric acid (65%) 0.285 mL (0.47 g, 10 mmol) was introduced. Following GC-MS monitoring of the reaction, the reaction mixture was carefully poured into ice water to induce solid precipitation. After thorough washing and filtration, the resultant filter cake was retained, and compound **4a** was obtained after drying. Compounds **4b** and **4c** were prepared using the same method.<sup>28</sup> Compounds **4a–4c** were used directly for the next step without any purification.

*General Synthetic Procedure for 5a–5c.* Compound **4a** (3.55 g, 10 mmol) was dissolved in ethanol (20 mL), and an aqueous solution of ammonium chloride (1.07 g, 20 mmol) was subsequently added. Reduced iron powder (1.68 g, 30 mmol) was introduced in three

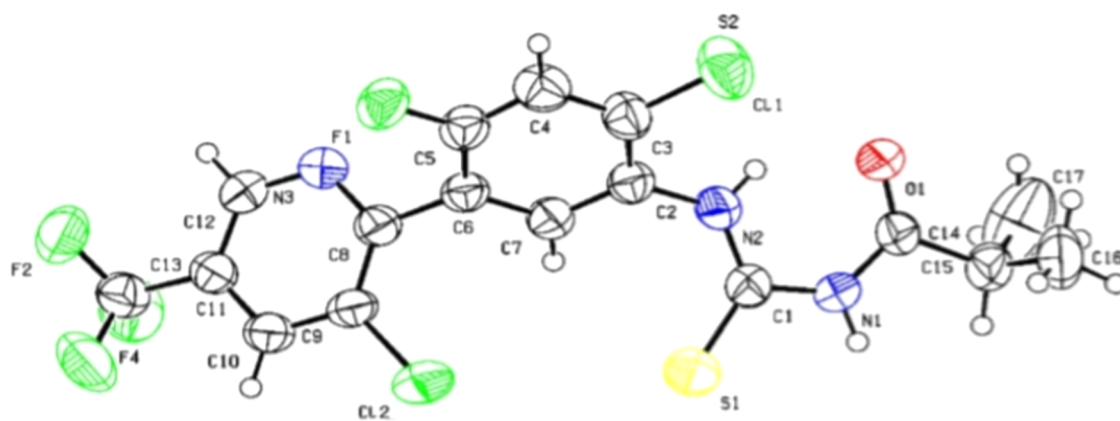


**Figure 2.** X-ray crystal structure of compound **8c**.

portions. After the completion of the reaction, as monitored by GC-MS, diatomaceous earth was used to filter out the iron powder. Ethanol was then evaporated. The reaction mixture was further subjected to extraction using salt water and ethyl acetate, retaining the organic layer. The solvent was evaporated, and compound **5a** was obtained through column chromatography. Compounds **5b** and **5c** were synthesized using the same method.<sup>29</sup> The <sup>1</sup>H NMR characterization data for compounds **5a–5c** are provided in the [Supporting Information](#).

**General Synthetic Procedure for 6a–6h.** In a round-bottom flask (50 mL), compound **5a** (325 mg, 1 mmol), the corresponding substituted acyl chloride (138 mg, 1.5 mmol), and triethylamine (202 mg, 2 mmol) were sequentially introduced into dichloromethane (10 mL). The mixture was stirred at 25 °C for the duration of the reaction. Once the reaction was concluded, the solvent was evaporated by steaming it out and the mixture was subsequently subjected to column chromatography for the isolation of compounds **6a**. Compounds **6b–6h** were synthesized using the same method.<sup>30</sup> The <sup>1</sup>H, <sup>13</sup>C, <sup>19</sup>F NMR, and HRMS characterization data for compounds **6a–6h** are provided in the [Supporting Information](#).

**General Synthetic Procedure for 7a–7o.** Compound **5a** (325 mg, 1 mmol) in a round-bottom flask (50 mL) was added to isocyanate (85.6 mg, 1.5 mmol) and dissolved in dichloromethane (10 mL) and then stirred at 25 °C. After the reaction was completed, the solvent was steamed out and separated through column chromatography to obtain compound **7a**. Compounds **7b–7o** were synthesized using the same method.<sup>31</sup> The <sup>1</sup>H, <sup>13</sup>C, <sup>19</sup>F NMR, and HRMS characterization data for compounds **7a–7o** are provided in the [Supporting Information](#).

**General Synthetic Procedure for 8a–8j.** Compound **5a** (325 mg, 1 mmol), an appropriate substituted acyl chloride (118 mg, 1.5 mmol), and ammonium thiocyanate (100 mg, 1.3 mmol) were sequentially introduced into a round-bottom flask (50 mL). These compounds were dissolved in 10 mL of acetone solvent, and the mixture was heated to 70 °C while stirring for the reaction. Upon the completion of the reaction, the solvent was evaporated and the resulting mixture was separated through column chromatography to yield compound **8a**. Compounds **8b–8j** were prepared using the same method.<sup>32</sup> The <sup>1</sup>H, <sup>13</sup>C, <sup>19</sup>F NMR, and HRMS characterization data for compounds **8a–8j** are provided in the [Supporting Information](#).

**X-ray Diffraction.** To elucidate the structure of the synthesized compound, X-ray structural analysis was performed using a single crystal of compound **8c**. The single crystal of compound **8c** was obtained by allowing dichloromethane to slowly evaporate. The X-ray crystal structure of compound **8c** is depicted in [Figure 2](#). Crystallographic data for crystal compound **8c** has been deposited at the Cambridge Crystallography Data Center (CCDC) under deposition number 2262927. These data were freely accessible at <https://www.ccdc.cam.ac.uk>.

**Herbicide Activity Assay.** Six representative weed species *Lolium perenne* (LP), *Echinochloa crus-galli* (EC), *Digitaria sanguinalis* (DS),

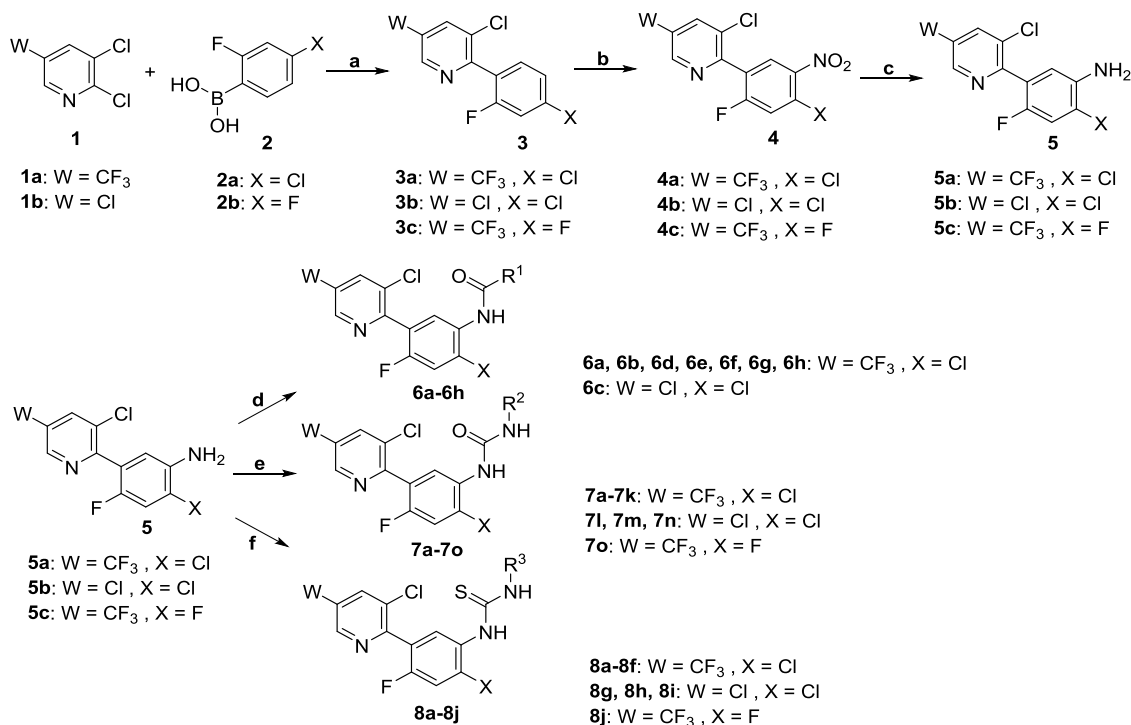
*Abutilon theophrasti* (AT), *Amaranthus retroflexus* (AR), and *Medicago sativa* (MS) were selected to assess the postemergence herbicidal activity of the compounds **6a–8j**. When weeds grew to 2–3 leaves stage, weeds exhibiting consistent uniformity, size, and development were chosen as test subjects. The target compounds **6a–8j** were dissolved respectively in 1 mL of *N,N*-dimethylformamide (DMF) at a concentration of 20 mg, creating a mother solution of 20 g/L. These solutions were further diluted using a 0.1% Tween-80 solution to achieve the desired concentration for spraying, following the established methods in the literature. The positive control employed was acifluorfen, while unapplied weeds served as the blank control. After 14 days, the herbicidal activity (inhibition rate %) of the compound-treated weeds was evaluated by visual method. The experiment was repeated three times for each test concentration.<sup>33</sup>

**Crop Selectivity Test.** Six representative crops such as corn, rice, wheat, peanut, cotton, and soybean seeds were utilized to conduct crop selectivity tests for the synthesized compounds **6a–8j**. The postemergence crop selectivity tests were performed at rates of 75 and 150 g ai/ha when the crops reached an appropriate growth stage (typically the four-leaf stage) as per the established methods.<sup>34</sup> After the application of the compounds through spraying, with acifluorfen employed as the positive control and untreated crops as the blank control, the treated crops were assessed for their crop selectivity (expressed as the inhibition rate %) after 3 weeks. Each tested concentration was replicated three times in the experimental setup.

**NtPPO Inhibitory Activity.** The inhibitory effect on NtPPO of **6a**, **7b**, **8d**, and commercial drug acifluorfen was tested *in vitro* through the use of the NtPPO enzyme-linked immunoassay test kit obtained from Jiangsu Meimian Industrial Co., Ltd. (Jiangsu Province, China). Each experiment was repeated three times independently. The experimental procedures were conducted following the instructions provided by the manufacturer, and the detailed steps of the experiments were in accordance with the previous reports.<sup>35</sup>

**Molecular Docking.** The crystal structure of NtPPO (PDB code 1SEZ) was downloaded from the Protein Data Bank (PDB) database. Compounds **6a**, **7b**, and **8d** were used for subsequent molecular dynamics (MD) simulation studies. The structures of compounds **6a**, **7b**, and **8d** were constructed and optimized using Chem3D 20.0 prior to their utilization. AutoDockTools version 1.5.6 was employed to prepare the ligands and receptors, and AutoDock 4.2 was utilized to predict the binding modes of compounds **6a**, **7b**, and **8d** with NtPPO. The receptor was extracted, and the simulation results were visualized using PYMOL.<sup>36</sup>

**MD Simulations.** The AMBER 14 software package, utilizing the ff14SB force fields, was employed to conduct MD simulations of the systems involving compounds **6a**, **7b**, and **8d**. The structures of the ligand–protein systems were analyzed at the 20 ns mark of the MD simulation using the CPPTRAJ module. The final 10 ns of the MD trajectories were utilized for energy decomposition analysis and the calculation of binding energy.<sup>35,36</sup>

Scheme 1. Synthesis of Compounds 6a–6h, 7a–7o, and 8a–8j<sup>a</sup>

<sup>a</sup>Reagents and conditions: (a) Pd(PPh<sub>3</sub>)<sub>2</sub>Cl<sub>2</sub>, Na<sub>2</sub>CO<sub>3</sub>, 1,2-dimethoxyethane/H<sub>2</sub>O = 1/1, 60 °C; (b) HNO<sub>3</sub>, H<sub>2</sub>SO<sub>4</sub>, 0 °C–r.t.; (c) Fe, NH<sub>4</sub>Cl, C<sub>2</sub>H<sub>5</sub>OH (80%), reflux; (d) R<sup>1</sup>COCl, Et<sub>3</sub>N, DCM, r.t.; (e) R<sup>2</sup>NCO, DCM, r.t.; and (f) R<sup>3</sup>COCl, NH<sub>4</sub>SCN, acetone, 70 °C.

Table 1. Chemical Structure and Postemergence Herbicidal Activity of Compounds 6a–6h

compounds	dosage (g ai/ha)	W	X	R <sup>1</sup>	% inhibition <sup>a</sup>					
					LP	EC	DS	AT	AR	MS
<b>6a</b>	150	CF <sub>3</sub>	Cl	CH <sub>2</sub> CH <sub>3</sub>	E	B	A	A	A	A
	75				G	E	C	A	A	A
	37.5				G	F	D	A	A	B
<b>6b</b>	150	CF <sub>3</sub>	Cl	CH(CH <sub>3</sub> ) <sub>2</sub>	D	B	A	A	A	A
	75				F	C	C	A	A	A
	37.5				G	D	D	A	A	A
<b>6c</b>	150	Cl	Cl	CH(CH <sub>3</sub> ) <sub>2</sub>	D	B	A	A	A	A
	75				E	E	B	B	A	B
	37.5				G	F	C	B	A	B
<b>6d</b>	150	CF <sub>3</sub>	Cl	CHCH <sub>2</sub>	G	G	G	B	A	B
<b>6e</b>	150	CF <sub>3</sub>	Cl	CH <sub>2</sub> Br	D	E	C	A	A	C
<b>6f</b>	150	CF <sub>3</sub>	Cl	CHCHC <sub>6</sub> H <sub>5</sub>	F	G	D	A	A	C
<b>6g</b>	150	CF <sub>3</sub>	Cl	4-NO <sub>2</sub> -C <sub>6</sub> H <sub>4</sub>	G	G	G	C	B	D
<b>6h</b>	150	CF <sub>3</sub>	Cl	4-OCH <sub>3</sub> -C <sub>6</sub> H <sub>4</sub>	G	G	G	A	D	D
acifluorfen	150				D	C	B	A	A	A
	75				F	D	D	B	A	C
	37.5				G	F	E	D	A	E

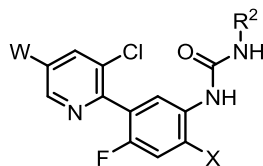
<sup>a</sup>Rating system for the growth inhibition percentage: A, ≥90%; B, 80–89%; C, 60–79%; D, 40–59%; E, 20–39%; F, 10–19%; and G, <10%. LP, *Lolium perenne*; EC, *Echinochloa crus-galli*; DS, *Digitaria sanguinalis*; AT, *Abutilon theophrasti*; AR, *Amaranthus retroflexus*; MS, *Medicago sativa*.

**Degradation Study of Compound 8d in AT.** We selected AT weeds with a growth period of 21 days for this experiment by utilizing the same application method as the “Herbicide Activity Assay”. Compound 8d was sprayed at a concentration of 150 g ai/ha. After the leaf surfaces dried, leaves were harvested at time intervals of 2, 6,

12, 24, 48, and 72 h. For each time point, 1.0 g of leaf samples were collected for subsequent analysis. The collected leaves for each period were ground in a mortar using liquid nitrogen, followed by the addition of 5 mL of methanol solution. Subsequently, 0.4 g of sodium chloride and 0.8 g of anhydrous sodium sulfate were added, and the



Table 2. Chemical Structure and Postemergence Herbicidal Activity of Compounds 7a–7o



compounds	dosage (g ai/ha)	W	X	R <sup>2</sup>	% inhibition <sup>a</sup>					
					LP	EC	DS	AT	AR	MS
7a	150	CF <sub>3</sub>	Cl	CH <sub>3</sub>	F	E	E	A	A	E
7b	150	CF <sub>3</sub>	Cl	C <sub>2</sub> H <sub>5</sub>	G	F	A	A	A	B
	75				G	G	C	A	A	C
	37.5				G	G	D	B	A	D
7c	150	CF <sub>3</sub>	Cl	CH <sub>2</sub> CH <sub>2</sub> CH <sub>3</sub>	F	E	C	A	A	E
7d	150	CF <sub>3</sub>	Cl	CH <sub>2</sub> CH <sub>2</sub> CH <sub>2</sub> CH <sub>3</sub>	G	F	D	B	A	E
7e	150	CF <sub>3</sub>	Cl	CH(CH <sub>3</sub> ) <sub>2</sub>	G	F	E	A	A	B
	75				G	G	F	B	A	C
	37.5				G	G	G	C	A	D
7f	150	CF <sub>3</sub>	Cl	2-Cl-C <sub>6</sub> H <sub>4</sub>	G	G	E	A	B	D
7g	150	CF <sub>3</sub>	Cl	4-Cl-C <sub>6</sub> H <sub>4</sub>	F	G	E	A	A	A
	75				G	G	E	B	B	B
	37.5				G	G	F	B	C	C
7h	150	CF <sub>3</sub>	Cl	3-OCH <sub>3</sub> -C <sub>6</sub> H <sub>4</sub>	G	F	E	A	B	D
7i	150	CF <sub>3</sub>	Cl	4-OCH <sub>3</sub> -C <sub>6</sub> H <sub>4</sub>	G	F	F	C	B	G
7j	150	CF <sub>3</sub>	Cl	3-CH <sub>3</sub> -C <sub>6</sub> H <sub>4</sub>	F	F	E	C	B	G
7k	150	CF <sub>3</sub>	Cl	4-CH <sub>3</sub> -C <sub>6</sub> H <sub>4</sub>	F	F	E	C	B	G
7l	150	Cl	Cl	C <sub>2</sub> H <sub>5</sub>	G	D	C	A	A	E
7m	150	Cl	Cl	CH <sub>2</sub> CH <sub>2</sub> CH <sub>3</sub>	G	F	E	C	A	F
7n	150	Cl	Cl	CH(CH <sub>3</sub> ) <sub>2</sub>	G	F	E	B	A	E
7o	150	CF <sub>3</sub>	F	2-Cl-C <sub>6</sub> H <sub>4</sub>	G	G	F	D	B	G
acifluorfen	150				D	C	B	A	A	A
	75				F	D	D	B	A	C
	37.5				G	F	E	D	A	E

<sup>a</sup>Rating system for the growth inhibition percentage: A, ≥90%; B, 80–89%; C, 60–79%; D, 40–59%; E, 20–39%; F, 10–19%; and G, <10%. LP, *Lolium perenne*; EC, *Echinochloa crus-galli*; DS, *Digitaria sanguinalis*; AT, *Abutilon theophrasti*; AR, *Amaranthus retroflexus*; MS, *Medicago sativa*.

mixture was vortexed for 5 min and then subjected to 30 min of ultrasonication. A 3 mL aliquot of the supernatant was taken and combined with 60 mg of the purification agent ethylenediamine n-propyl silane (PSA) and 60 mg of octadecylsilane-bonded silica gel (C18). After vortexing for 5 min, the mixture was sonicated for an additional 30 min. The resulting supernatant was collected, passed through a 0.22 μm organic membrane filter, and prepared for LC-MS analysis.<sup>37</sup>

## RESULTS AND DISCUSSION

**Synthesis.** The synthetic routes for compounds 6a–6h, 7a–7o, and 8a–8j are depicted in Scheme 1. Briefly, various substituted 2-chloropyridines (1a–1b) and phenylboronic acids (2a–2b) with diverse substituent groups were employed as starting materials. This led to the formation of the pyridine phenyl structure (3a–3c) through coupling reactions. The reaction is catalyzed by Pd(PPh<sub>3</sub>)<sub>2</sub>Cl<sub>2</sub> and occurs under alkaline conditions using Na<sub>2</sub>CO<sub>3</sub> as a base. The solvent is a mixture of volume ratios, with V(1,2-dimethoxyethane)/V(H<sub>2</sub>O) = 1/1, and the reaction is conducted at a temperature of 60 °C. Subsequently, compounds 4a–4c are obtained through a nitration reaction, wherein a nitro group is selectively introduced onto the phenyl moiety of 3a–3c under carefully controlled conditions maintained between 0 and 5 °C. Compounds 4a–4c were used directly for the next step without purification. Compounds 4a–4c are subjected to acidic conditions provided by reducing iron powder and

ammonium chloride, leading to the reduction of nitro groups to amino groups and yielding compounds 5a–5c. Compounds 6a–6h were prepared from 5a–5c and various substituted acyl chlorides (R<sup>1</sup>COCl) in the presence of triethylamine (Et<sub>3</sub>N) as a base. Compounds 7a–7o were prepared from the reaction between the pyridine aniline structure (5a–5c) and the corresponding isocyanates (R<sup>2</sup>NCO). Compounds 8a–8j were synthesized by subjecting diverse substituted acyl chlorides (R<sup>3</sup>COCl) to the corresponding solution of 5a–5c and NH<sub>4</sub>SCN in acetone at 70 °C. The compounds were characterized by <sup>1</sup>H NMR, <sup>13</sup>C NMR, and <sup>19</sup>F NMR spectra and HRMS. Detailed spectra results for all compounds are provided in the Supporting Information.

**Herbicidal Activity.** As shown in Tables 1–3, the results indicated that compounds 6a–8j exhibit an overall superior postemergence herbicidal activity against broadleaf weeds compared to monocotyledon weeds. Some compounds such as 6a, 6b, 6c, 7b, 8a, 8c, 8d, and 8h exhibited significant postemergence herbicidal activity, demonstrating effective control over broadleaf weeds when compared to acifluorfen.

We observed that compound 8d exhibited a significant level of herbicidal activity when compared to acifluorfen. When applied at a dosage of 150 g ai/ha, compound 8d demonstrates a slightly elevated control over EC in comparison to acifluorfen. Moreover, compound 8d shows comparable control over other weed species such as DS, AR, MS, and

Table 3. Chemical Structure and Postemergence Herbicidal Activity of Compounds 8a–8j

compounds	dosage (g ai/ha)	W	X	R <sup>3</sup>	% inhibition <sup>a</sup>						
					LP	EC	DS	AT	AR	MS	
<b>8a</b>	150	CF <sub>3</sub>	Cl	COCH <sub>3</sub>	D	D	B	A	A	A	
	75				D	D	B	A	A	A	
	37.5				E	E	B	A	A	D	
<b>8b</b>	150	CF <sub>3</sub>	Cl	COC <sub>2</sub> H <sub>5</sub>	F	E	C	A	A	D	
	<b>8c</b>	150	CF <sub>3</sub>	Cl	COCH(CH <sub>3</sub> ) <sub>2</sub>	D	D	A	A	A	A
		75				E	E	C	A	A	A
<b>8d</b>	150	CF <sub>3</sub>	Cl	COC(CH <sub>3</sub> ) <sub>3</sub>	D	B	A	A	A	A	
	75				E	C	C	A	A	A	
	37.5				F	D	D	A	A	A	
<b>8e</b>	150	CF <sub>3</sub>	Cl	COOC <sub>2</sub> H <sub>5</sub>	F	E	D	A	A	F	
<b>8f</b>	150	CF <sub>3</sub>	Cl	4-NO <sub>2</sub> -C <sub>6</sub> H <sub>4</sub>	F	G	C	A	A	G	
<b>8g</b>	150	Cl	Cl	COC <sub>2</sub> H <sub>5</sub>	E	E	D	A	A	B	
<b>8h</b>	150	Cl	Cl	COCH(CH <sub>3</sub> ) <sub>2</sub>	E	D	A	A	A	A	
	75				F	F	C	A	A	B	
	37.5				G	E	C	B	A	C	
<b>8i</b>	150	Cl	Cl	COOC <sub>2</sub> H <sub>5</sub>	G	F	F	B	B	G	
<b>8j</b>	150	CF <sub>3</sub>	F	COCH <sub>3</sub>	F	E	E	A	A	A	
acifluorfen	150				D	C	B	A	A	A	
	75				F	D	D	B	A	C	
	37.5				G	F	E	D	A	E	

<sup>a</sup>Rating system for the growth inhibition percentage: A, ≥90%; B, 80–89%; C, 60–79%; D, 40–59%; E, 20–39%; F, 10–19%; and G, <10%. LP, *Lolium perenne*; EC, *Echinochloa crus-galli*; DS, *Digitaria sanguinalis*; AT, *Abutilon theophrasti*; AR, *Amaranthus retroflexus*; MS, *Medicago sativa*.

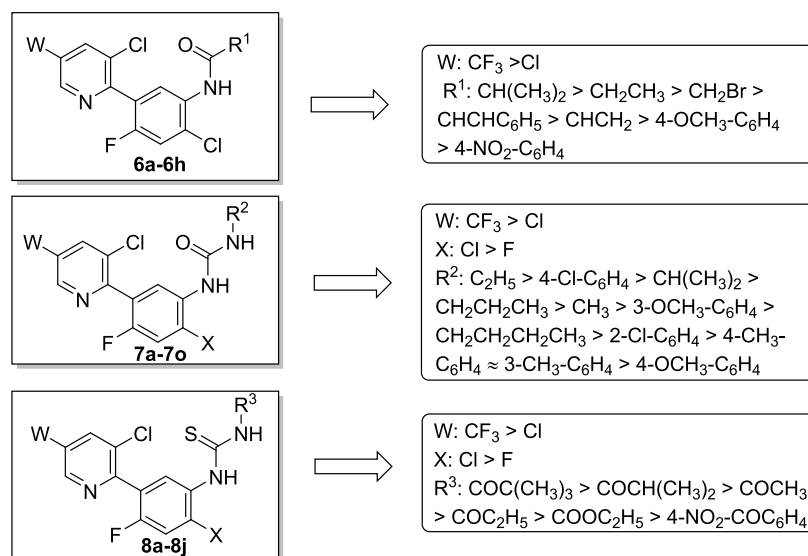


Figure 3. Relationship between structure and herbicidal activity of compounds 6a–8j.

AT as seen with acifluorfen. However, it is worth noting that compound **8d** exhibits a slightly diminished level of control over LP when contrasted with acifluorfen. Upon reducing the application dosage, we were delighted to find that the herbicidal activity of compound **8d** remained effective against AR, AT, and MS, even at a lower dosage of 75 g ai/ha. Impressively, compound **8d** displays robust efficacy in

controlling these weeds at a concentration as low as 37.5 g ai/ha. The herbicidal activity of **8d** against broadleaf weeds continues to maintain an excellent level of effectiveness when compared to acifluorfen. It is worth noting that replacing the pyridine unit of compound **8d** with phenyl (named **8k**) results in significantly dropped herbicidal activity (see Table S3 for details).



**Figure 4.** Postemergence Crop Selectivity of Acifluorfen and Compound **8d** (150 g ai/ha, 14 Days after Spraying). Crop names from left to right: corn, rice, wheat, peanut, cotton, soybean.

**Structure–Activity Relationship.** The structure–activity relationship of these compounds is summarized in Figure 3. The results suggested that compounds with pyridine ring bearing  $\text{CF}_3$  group ( $W = \text{CF}_3$ ) generally exhibit higher herbicidal activity compared with Cl-substituted ones ( $W = \text{Cl}$ ). The introduction of  $\text{CF}_3$  remarkably enhances the herbicidal efficacy of the compounds when compared to Cl. In addition, the effect of the substituent X on the benzene ring also proves significant. For example, the herbicidal activity experienced a notable increase when an F atom was replaced by a Cl atom.

As shown in Table 1, the  $\text{R}^1$  group in **6a–6h** also shows a remarkable effect on the herbicidal activity. Generally, compounds bearing a saturated alkyl group exhibit higher levels of herbicidal activity than those bearing vinyl or aryl groups. Specifically, when the substituent at  $\text{R}^1$  is  $\text{CH}(\text{CH}_3)_2$  (**6b**), the herbicidal activity is marginally superior to that observed when the substituent at  $\text{R}^1$  is  $\text{CH}_2\text{CH}_3$  (**6a**). Meanwhile, when there is significant steric hindrance at the  $\text{R}^1$  position, the herbicidal activity is decreased. For instance, the herbicidal activity of compound **6f**, in which the  $\text{R}^1$  group is a phenyl group, is obviously less active than compound **6a** bearing an alkyl group as the  $\text{R}^1$  group. Additionally, when the substituent at the  $\text{R}^1$  position is a substituted benzene ring, the substituent attached to the benzene ring has an obvious influence on the herbicidal activity. Furthermore, in cases where an electron-rich group is installed (**6h**), the herbicidal activity is slightly higher than that of those bearing an electron-deficient group (**6g**).

The herbicidal activities of compounds **7a–7o** are listed in Table 2. The results revealed that the herbicidal activity is sensitive to the  $\text{R}^2$  group. An obvious improvement in the herbicidal activity was observed when an aryl group was replaced by a saturated alkyl group. Notably, among all of the tested alkyl groups (**7a–7e**),  $\text{C}_2\text{H}_5$  (**7b**) showed the highest level of herbicidal activities for most of the tested weeds. When  $\text{R}^2$  is an aryl group, both the electronic and steric effects of the substituent obviously impact the herbicidal activity. For instance, the 4-Cl group on the phenyl ring (**7g**) exhibited better herbicidal activities than the 4-methyl (**7k**), 4-methoxyl (**7i**), and 2-Cl groups (**7f**). The 4-methoxyl group on the phenyl ring (**7i**) led to higher herbicidal activity than the 3-methoxyl group (**7h**).

The detailed structure–activity relationship of **8a–8j** listed in Table 3 reveals that acyl groups (**8a–8d**) as  $\text{R}^3$  generally exhibited higher herbicidal activities than those bearing alkoxycarbonyl (**8e**) or aryl (**8f**) groups. Specifically, among the tested acyl groups such as  $\text{COCH}_3$  (**8a**),  $\text{COC}_2\text{H}_5$  (**8b**),  $\text{COCH}(\text{CH}_3)_2$  (**8c**), and  $\text{COC}(\text{CH}_3)_3$  (**8d**), **8d** bearing a *t*-Bu group showed the highest herbicidal activity. Compounds

bearing  $\text{COOC}_2\text{H}_5$  (**8e**) and  $4\text{-NO}_2\text{-C}_6\text{H}_4$  (**8f**) as the  $\text{R}^3$  demonstrate similar herbicidal activities.

Furthermore, it can be inferred that introducing thiourea fragments into the herbicide structure led to more favorable interactions between the compound and the receptor, which would be beneficial for enhancing the compound's herbicide activity.

**Crop Selectivity.** To demonstrate the safety of our designed compounds for the crops, **6a**, **7b**, and **8d** were chosen as representative examples to test the crop selectivity at both 150 and 75 g ai/ha dosages through a 14-day period. After being treated with compounds **6a**, **7b**, and **8d**, mild burning symptoms were observed during the first few days on the leaves of monocotyledonous crops (corn, rice, and wheat). However, all these three crops were able to repair this initial damage after 5 days of application (Figure 4 and Table 4),

**Table 4.** Postemergence Crop Selectivity of Compounds **6a**, **7b**, **8d**, and Acifluorfen

compounds	dosage (g ai/ha)	% inhibition <sup>a</sup>					
		corn	rice	wheat	peanut	cotton	soybean
<b>6a</b>	150	G	G	G	G	F	F
	75	G	G	G	G	G	G
<b>7b</b>	150	G	G	G	G	F	F
	75	G	G	G	G	G	G
<b>8d</b>	150	G	G	G	F	E	D
	75	G	G	G	G	F	E
acifluorfen	150	G	G	G	G	B	E
	75	G	G	G	G	D	F

<sup>a</sup>Rating system for the growth inhibition percentage: A,  $\geq 90\%$ ; B, 80–89%; C, 60–79%; D, 40–59%; E, 20–39%; F, 10–19%; and G,  $< 10\%$ .

suggesting that the compounds **6a**, **7b**, and **8d** exhibited excellent selectivity for monocotyledonous crops at a dosage of 75–150 g ai/ha. Moreover, the crop selectivity studies revealed that compounds **6a** and **7b** exhibited crop safety comparable or even superior to that of the commercial herbicide acifluorfen. Although compound **8d** demonstrated limited selectivity toward peanuts and soybeans, it exhibited superior selectivity for cotton compared to acifluorfen at a dosage of 75–150 g ai/ha. Hence, the research results indicate that compound **8d**, which possesses strong herbicidal activity, holds the potential to serve as a postemergence herbicide for the fields of wheat, corn, peanuts, and cotton.

**PPO Inhibitory Activity.** To provide evidence supporting our compounds as PPO inhibitors, the inhibitory effect of compounds **6a**, **7b**, and **8d** on the activity of *Nt*PPO was

Table 5. *Nt*PPO Inhibition Activity of Compounds 6a, 7b, 8d, and Acifluorfen

compounds	6a	7b	8d	acifluorfen
$IC_{50}$ ( $\mu M$ ) <sup>a</sup>	0.382 $\pm$ 0.0022	1.079 $\pm$ 0.0017	0.1903 $\pm$ 0.0016	1.376 $\pm$ 0.0018

<sup>a</sup>Values are expressed as mean  $\pm$  standard deviation.

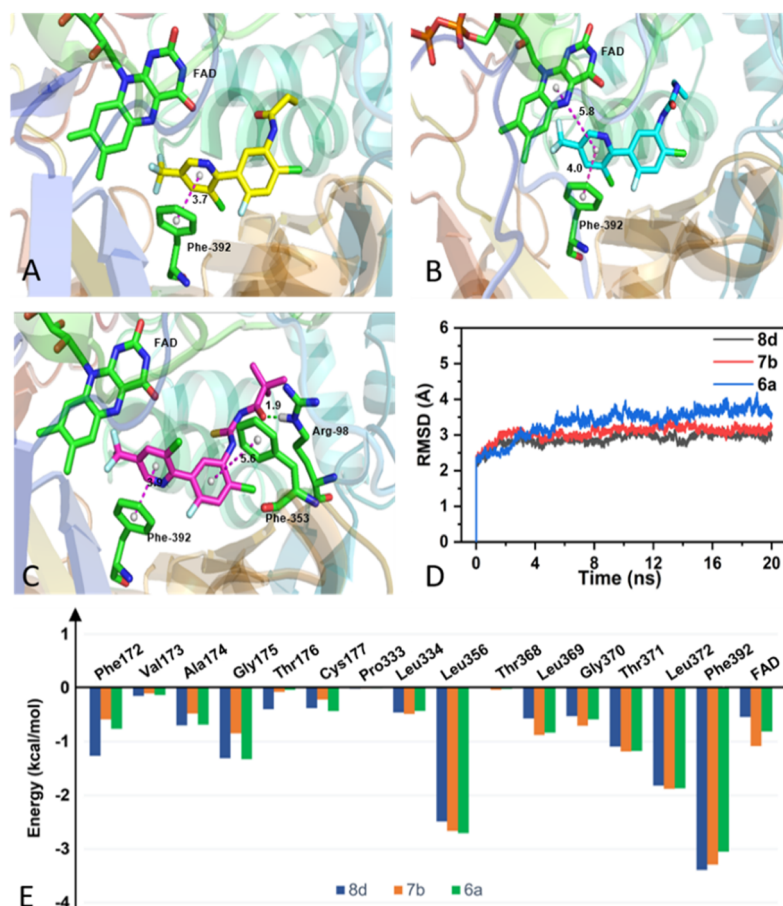


**Figure 5.** Molecular docking results of compounds 6a, 7b, and 8d with *Nt*PPO. The inhibitors are shown as yellow, blue, and magenta sticks, and the key residues around the active site are shown as green sticks. (A) Binding mode of compound 6a with *Nt*PPO. (B) Binding mode of compound 7b with *Nt*PPO. (C) Binding mode of compound 8d with *Nt*PPO. (D) RMSD of backbone atoms of protein. (E) Comparison of the total interaction binding energies (kcal/mol) between compounds 6a, 7b, 8d, and *Nt*PPO.

investigated, and the results are summarized in Table 5. The half-maximal inhibitory concentration ( $IC_{50}$ ) values of compounds 6a, 7b, and 8d were tested as 0.38, 1.08, and 0.19  $\mu M$ , respectively, which are lower than those of the commercial acifluorfen ( $IC_{50} = 1.38 \mu M$ ). In addition, among the tested compounds (6a, 7b, and 8d), 8d showed the lowest  $IC_{50}$  value, suggesting the highest inhibitory activity of 8d toward *Nt*PPO. This result was consistent with the data of experimental herbicidal activities, revealing that the enhancement of the herbicidal activities of thiourea is higher than that of urea and amide motifs. Overall, the inhibitory effect of our compounds supports them to act as PPO inhibitors.

**Molecular Docking Studies.** To elucidate the interaction modes and binding conformations between the compounds and *Nt*PPO, molecular docking studies were conducted by using compounds 6a, 7b, and 8d as ligands and *Nt*PPO as the receptor. The results are summarized in Figure 5. Specifically, it was found that there is a clear  $\pi$ - $\pi$  interaction between the pyridine ring of compound 6a and phenylalanine (Phe-392) (Figure 5A). For compound 7b, the pyridine ring interacts with both the phenylalanine (Phe-392) and the flavin adenine

dinucleotide (FAD) via  $\pi$ - $\pi$  stacking interaction (Figure 5B). Compared to 6a and 7b, compound 8d can provide multi-interaction sites and different interaction models with *Nt*PPO. Specifically, the benzene ring and pyridine ring of 8d interacts with the phenylalanine (Phe-353) and phenylalanine (Phe-392) via  $\pi$ - $\pi$  interactions, respectively (Figure 5C). In addition, the oxygen atom in the thiourea chain of 8d forms a hydrogen bond interaction with the adjacent arginine (Arg-98) with a hydrogen bond length of 1.9 Å (Figure 5C). Such a hydrogen bond interaction was not formed with compounds 6a and 7d due to the orientations of oxygen atoms. Therefore, the higher quantity and diverse type of interactions between 8d and the residues within the active site pocket provide an efficient binding mode with *Nt*PPO, which would enhance its affinity to *Nt*PPO and exhibit improved herbicidal activities. Such molecular docking results are consistent with our experimental observations.

**MD Simulations.** To gain more insight into the inhibition mechanism, molecular dynamic (MD) simulations between 6a, 7b, and 8d and *Nt*PPO were conducted. As the main variation of the structure for these three target molecules comes from



the side chain, we focused our attention on investigating the effect induced by the side chain on the pyridine ring. As shown in Figure 5D, over a 20 ns MD simulation period, all root-mean-square-deviation (RMSD) values of backbone atoms of protein are concentrated around 2.5–3.5 Å at the last 10 ns, indicating that the 6a-*Nt*PPO, 7b-*Nt*PPO, and 8d-*Nt*PPO systems have reached stability. Further energy decomposition study also supports this result. Specifically, the experiment revealed that the energy contribution of phenylalanine (Phe-392) to compound 8d was higher (−3.40 kcal/mol) than that to compound 7b (−3.30 kcal/mol) and 6a (−3.02 kcal/mol) (Figure 5E). Overall, MD simulation studies demonstrated that the presence of thiourea chains enhances the interaction between 8d and *Nt*PPO, resulting in higher affinity and herbicidal activities. Meanwhile, the binding free energy ( $\Delta G_{\text{bind}}$ ) of compounds 8d with *Nt*PPO was calculated as −24.09 kcal/mol, suggesting that compound 8d bonded more tightly with *Nt*PPO than compounds 6a (−15.65 kcal/mol) and 7b (−9.55 kcal/mol) (for more detailed information, see Table S2). These results were consistent with the PPO inhibition experiments.

**In Vivo Degradation Study of 8d.** The *in vivo* degradation of 8d was also explored by using UPLC-HRMS. AT was chosen as the experimental weed for the degradation study. The LC-MS test results listed in Figure 6 and Table S1

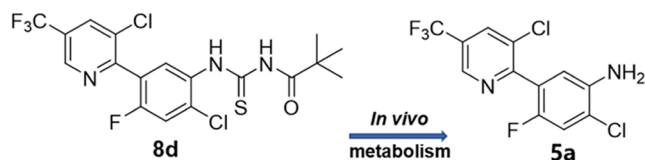
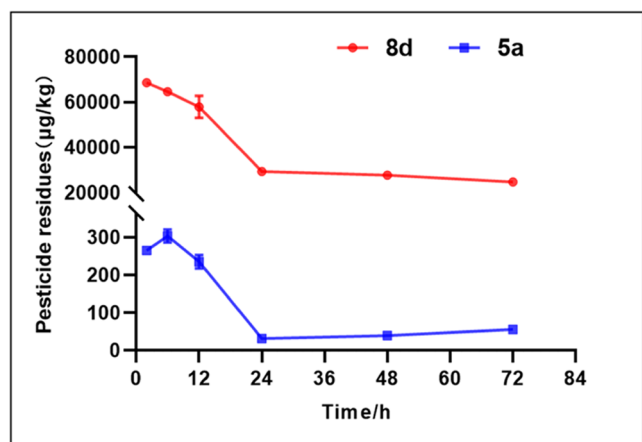


Figure 6. Degradation study of compound 8d in *A. theophrasti*.

revealed that compound 8d existed in the AT decomposed to compound 5a within the first 24 h. However, the decomposition of 8d almost stopped after 24 h since only a slight decrease in the concentration of 8d was observed after 24 h. Meanwhile, the concentration of 5a increased rapidly at the beginning and reached a peak value after 6 h. Then, the concentration started to decrease, and the minimum concentration appeared at 24 h. In the following time, a slight increase in the concentration of 5a was observed. It was found that the changing rates in the concentrations of 8d and 5a were related to the growth state of AT. Specifically, the leaves of AT gradually turned pale green after 24 h, then completely became white within 48 and 72 h, and ultimately died. Based on these

observations, we assumed that compound 8d would undergo hydrolysis to generate 5a in the biological system. Our results revealed that the main metabolite of compound 8d in plants is 5a, providing important information for further research on its environmental behavior and pesticide residues. In addition, the potential herbicidal activity of compound 5a against broad-leaved weeds (Table S4) suggests that 5a may be a meaningful intermediate for the development of new herbicides.

## CONCLUSIONS

In summary, we have designed and synthesized three types of substituted 3-(pyridin-2-yl)phenylamino derivatives via a structure splicing strategy. Herbicidal activity studies and crop selectivity evaluation of 33 newly prepared compounds revealed that these compounds exhibited good to excellent herbicidal activities and crop selectivity. Some of them such as 6a, 7b, and 8d exhibited superior herbicidal activities against broadleaf and monocotyledon weeds to commercial acifluorfen. Molecular simulation studies reveal that there are effective interactions between the tested compounds (6a, 7b, and 8d) and the amino acid residues of *Nt*PPO. These results were further supported by the *in vitro* *Nt*PPO inhibitory studies, demonstrating our compounds as typical PPO inhibitors. The high herbicidal activity and excellent crop safety of 8d demonstrated that it may be a promising candidate for novel herbicide development. Further studies including structural optimizations and mechanistic evaluations are ongoing in our laboratories.

## ASSOCIATED CONTENT

### Supporting Information

The Supporting Information is available free of charge at <https://pubs.acs.org/doi/10.1021/acs.jafc.3c06144>.

Detailed information for synthetic procedures, physical and spectrum data of all title compounds, degradation dynamics of compound 8d in *Abutilon theophrasti*, binding free energy calculations using the MM-PBSA method, postemergence herbicidal activity of compounds 8k, postemergence herbicidal activity of compounds 5a, calibration curves, and NMR spectra (PDF)

## AUTHOR INFORMATION

### Corresponding Authors

Shichao Ren – National Key Laboratory of Green Pesticide, Key Laboratory of Green Pesticide and Agricultural Bioengineering, Ministry of Education, Guizhou University, Guiyang 550025, People's Republic of China; [orcid.org/0000-0003-4248-6021](https://orcid.org/0000-0003-4248-6021); Email: [scren@gzu.edu.cn](mailto:scren@gzu.edu.cn)

Yonggui Robin Chi – National Key Laboratory of Green Pesticide, Key Laboratory of Green Pesticide and Agricultural Bioengineering, Ministry of Education, Guizhou University, Guiyang 550025, People's Republic of China; School of Chemistry, Chemical Engineering, and Biotechnology, Nanyang Technological University, Singapore 637371, Singapore; [orcid.org/0000-0003-0573-257X](https://orcid.org/0000-0003-0573-257X); Email: [robinchi@ntu.edu.sg](mailto:robinchi@ntu.edu.sg)

### Authors

Zhongyin Chen – National Key Laboratory of Green Pesticide, Key Laboratory of Green Pesticide and Agricultural

Bioengineering, Ministry of Education, Guizhou University, Guiyang 550025, People's Republic of China

**Hui Cai** – National Key Laboratory of Green Pesticide, Key Laboratory of Green Pesticide and Agricultural Bioengineering, Ministry of Education, Guizhou University, Guiyang 550025, People's Republic of China

**Xiao Zhang** – National Key Laboratory of Green Pesticide, Key Laboratory of Green Pesticide and Agricultural Bioengineering, Ministry of Education, Guizhou University, Guiyang 550025, People's Republic of China

**Meng Zhang** – National Key Laboratory of Green Pesticide, Key Laboratory of Green Pesticide and Agricultural Bioengineering, Ministry of Education, Guizhou University, Guiyang 550025, People's Republic of China

**Ge-Fei Hao** – National Key Laboratory of Green Pesticide, Key Laboratory of Green Pesticide and Agricultural Bioengineering, Ministry of Education, Guizhou University, Guiyang 550025, People's Republic of China; [orcid.org/0000-0003-4090-8411](https://orcid.org/0000-0003-4090-8411)

**Zhichao Jin** – National Key Laboratory of Green Pesticide, Key Laboratory of Green Pesticide and Agricultural Bioengineering, Ministry of Education, Guizhou University, Guiyang 550025, People's Republic of China

Complete contact information is available at:

<https://pubs.acs.org/10.1021/acs.jafc.3c06144>

## Notes

The authors declare no competing financial interest.

## ACKNOWLEDGMENTS

The authors acknowledge financial support from the National Natural Science Foundation of China (22371058, 21961006, 32172459, 22371057, and 22071036), the starting grant of Guizhou University [(2023)29], the National Natural Science Fund for Excellent Young Scientists Fund Program (Overseas), the Science and Technology Department of Guizhou Province (Qiankehejichu-ZK[2021]Key033), the Program of Introducing Talents of Discipline to Universities of China (111 Program, D20023) at Guizhou University, Frontiers Science Center for Asymmetric Synthesis and Medicinal Molecules, Department of Education, Guizhou Province [Qianjiaohu KY (2020)004], and Guizhou University (China).

## REFERENCES

- (1) Godfray, H. C. J.; Beddington, J.; Crute, I.; Haddad, L.; Lawrence, D.; Muir, J.; Pretty, J.; Robinson, S.; Thomas, S.; Toulmin, C. Food security: the challenge of feeding 9 billion people. *Science* **2010**, *327*, 812–818.
- (2) Oerke, E. C. Crop losses to pests. *J. Agric. Sci.* **2006**, *144*, 31–43.
- (3) Renton, M.; Busi, R.; Neve, P.; Thornby, D.; Vila-Aiub, M. Herbicide resistance modelling: past, present and future. *Pest Manage. Sci.* **2014**, *70*, 1394–1404.
- (4) Chauvel, B.; Guillemin, J. P.; Gasquez, J.; Gauvrit, C. History of chemical weeding from 1944 to 2011 in france: changes and evolution of herbicide molecules. *Crop Prot.* **2012**, *42*, 320–326.
- (5) Küpper, A.; Borgato, E. A.; Patterson, E. L.; Gonçalves Netto, A.; Nicolai, M.; Carvalho, S. J. P.; Nissen, S. J.; Gaines, T. A.; Christoffoleti, P. J. Multiple resistance to glyphosate and acetolactate synthase inhibitors in palmer amaranth (*amaranthus palmeri*) identified in Brazil. *Weed Sci.* **2017**, *65*, 317–326.
- (6) Délye, C. Weed resistance to acetyl coenzyme a carboxylase inhibitors: an update. *Weed Sci.* **2005**, *53*, 728–746.

(7) Green, J. M.; Owen, M. D. K. Herbicide-resistant crops: utilities and limitations for herbicide resistant weed management. *J. Agric. Food Chem.* **2011**, *59*, 5819–5829.

(8) Yuhan, Z.; Weirong, M.; Yibai, C.; Daxiang, W.; Su, B. Z. Research progress on protoporphyrinogen oxidase inhibitors and herbicides. *J. Pestic. Sci.* **2002**, *4*, 1–8.

(9) Zhao, L. X.; Chen, K. Y.; He, X. L.; Zou, Y. L.; Gao, S.; Fu, Y.; Ye, F. Design, synthesis, and biological activity determination of novel phenylpyrazole protoporphyrinogen oxidase inhibitor herbicides containing five-membered heterocycles. *J. Agric. Food Chem.* **2023**, *71*, 14164–14178.

(10) Zheng, B. F.; Zuo, Y.; Huang, G. Y.; Wang, Z. Z.; Ma, J. Y.; Wu, Q. Y.; Yang, G. F. Synthesis and biological activity evaluation of benzoxazinone-pyrimidinedione hybrids as potent protoporphyrinogen IX oxidase inhibitor. *J. Agric. Food Chem.* **2023**, *71*, 14221–14231.

(11) Liu, H. Y.; Yu, L. K.; Qin, S. N.; Yang, H. Z.; Wang, D. W.; Xi, Z. Design, synthesis, and metabolism studies of *N*-1,4-diketophenyl-triazinones as protoporphyrinogen IX oxidase inhibitors. *J. Agric. Food Chem.* **2023**, *71*, 3225–3238.

(12) Wang, B.; Wen, X.; Xi, Z. Molecular simulations bring new insights into protoporphyrinogen IX oxidase/protoporphyrinogen IX interaction modes. *Mol. Inf.* **2016**, *35*, 476–482.

(13) Brzezowski, P.; Ksas, B.; Havaux, M.; Grimm, B.; Chazaux, M.; Peltier, G.; Johnson, X.; Alric, J. The function of protoporphyrinogen IX oxidase in chlorophyll biosynthesis requires oxidised plastoquinone in *chlamydomonas reinhardtii*. *Commun. Biol.* **2019**, *2*, 159.

(14) Hess, F. D. Light-dependent herbicides: an overview. *Weed Sci.* **2000**, *48*, 160–170.

(15) Matringe, M.; Camadro, J. M.; Labbe, P.; Scalla, R. Protoporphyrinogen oxidase as a molecular target for diphenyl ether herbicides. *Biochem. J.* **1989**, *260*, 231–235.

(16) Duke, S. O.; Becerril, J. M.; Sherman, T. D.; Lydon, J.; Matsumoto, H. The role of protoporphyrin IX in the mechanism of action of diphenyl ether herbicides. *Pestic. Sci.* **1990**, *30*, 367–378.

(17) Schäfer, P.; Hamprecht, G.; Puhl, M.; Westphalen, K. O.; Zagar, C. Synthesis and herbicidal activity of phenylpyridines – a new lead. *Chimia* **2003**, *57*, 715–719.

(18) Jeschke, P. Latest generation of halogen-containing pesticides. *Pest Manage. Sci.* **2017**, *73*, 1053–1066.

(19) Fujiwara, T.; O'Hagan, D. Successful fluorine-containing herbicide agrochemicals. *J. Fluorine Chem.* **2014**, *167*, 16–29.

(20) Alnafta, N.; Beffa, R.; Bojack, G.; Bollenbach-Wahl, B.; Brant, N. Z.; Dörnbrack, C.; Dorn, N.; Freigang, J.; Gatzweiler, E.; Getachew, R.; Hartfel, C.; Heinemann, I.; Helmke, H.; Hohmann, S.; Jakobi, H.; Lange, G.; Lümmen, P.; Willms, L.; Frackenhohl, J. Designing new protoporphyrinogen oxidase-inhibitors carrying potential side chain isosteres to enhance crop safety and spectrum of activity. *J. Agric. Food Chem.* **2023**, *71*, 18270–18284.

(21) Yang, X.; Wang, H.; Jin, Z.; Chi, Y. R. Development of green and low-cost chiral oxidants for asymmetric catalytic hydroxylation of enals. *Green Synth. Catal.* **2021**, *2*, 295–298.

(22) Lv, Y.; Luo, G.; Liu, Q.; Jin, Z.; Zhang, X.; Chi, Y. R. Catalytic atroposelective synthesis of axially chiral benzonitriles via chirality control during bond dissociation and CN group formation. *Nat. Commun.* **2022**, *13*, No. 36.

(23) Lv, J.; Zou, J.; Nong, Y.; Song, J.; Shen, T.; Cai, H.; Mou, C.; Lyu, W.; Jin, Z.; Chi, Y. R. Catalytic regioselective acylation of unprotected nucleosides for quick access to COVID and other nucleoside prodrugs. *ACS Catal.* **2023**, *13*, 9567–9576.

(24) Hamm, P. C. Discovery, development, and current status of the chloroacetamide herbicides. *Weed Sci.* **1974**, *22*, 541–545.

(25) Berger, B. M.; Muller, M.; Eing, A. Quantitative structure-transformation relationships of phenylurea herbicides. *Pest Manage. Sci.* **2001**, *57*, 1043–1054.

(26) Tan, W.; Wei, J.; Jiang, X. Thiocarbonyl surrogate via combination of sulfur and chloroform for thiocarbamide and oxazolidinethione construction. *Org. Lett.* **2017**, *19*, 2166–2169.

(27) Dharman, P.; Babu, V.; Basha, K. A. Facile synthesis of novel 5-substituted pyridine 2 carboxamide derivatives and their biological

evaluation and 3D QSAR studies. *J. Chin. Chem. Soc.* **2019**, *66*, 415–426.

(28) Flohr, A.; Eidam, O.; Fasching, B.; Meniconi, M.; Sadok, A.; Chopra, R.; Zhuai Wang, H.; Caldwell, J. J.; Collins, I.; Ryckmans, T. Isoindolinone Compounds as Cereblon Inhibitors and GSPT1 Degradors and Their Preparation. WIPO Patent WO2021069705, 2021.

(29) Bryan, M. C.; Do, S.; Drobnick, J.; Gobbi, A.; Katsumoto, T.; Kiefer, J. R., Jr.; Liang, J.; Rajapaksa, N. S.; Chen, Y.; Fu, L.; Lai, K. W.; Liu, Z.; Wai, J.; Wang, F. Preparation of Pyrazolo [1,5a] Pyrimidine Derivatives as IRAK4 Modulators. WIPO Patent WO2018234345, 2018.

(30) Sadig, J. E. R.; Foster, R.; Wakenhut, F.; Michael, C. Palladium-catalyzed synthesis of benzimidazoles and quinazolinones from common precursors. *J. Org. Chem.* **2012**, *77*, 9473–9486.

(31) Lengyel, I.; Patel, H.; Ralph, J.; Stephani, A. The preparation and characterization of nineteen new phthalidyl spirohydantoin. *Heterocycles* **2007**, *73*, 349–375, DOI: 10.3987/COM-07-S(U)9.

(32) Zeng, R. S.; Zou, J. P.; Zhi, S. J.; Chen, J.; Shen, Q. Novel synthesis of 1-aryl-3-aryl-4-substituted imidazole-2-thiones. *Org. Lett.* **2003**, *5*, 1657–1659.

(33) Jiang, L. L.; Zuo, Y.; Wang, Z. F.; Tan, Y.; Wu, Q. Y.; Xi, Z.; Yang, G. F. Design and syntheses of novel *N*-(benzothiazol-5-yl)-4,5,6,7-tetrahydro-1*H*-isoindole-1,3(2*H*)-dione and *N*-(benzothiazol-5-yl) isoindoline-1,3-dione as potent protoporphyrinogen oxidase inhibitors. *J. Agric. Food Chem.* **2011**, *59*, 6172–6179.

(34) Zhao, L. X.; Jiang, M. J.; Hu, J. J.; Zou, Y. L.; Cheng, Y.; Ren, T.; Gao, S.; Fu, Y.; Ye, F. Design, synthesis, and herbicidal activity of novel diphenyl ether derivatives containing fast degrading tetrahydrophthalimide. *J. Agric. Food Chem.* **2020**, *68*, 3729–3741.

(35) Wang, D. W.; Liang, L.; Xue, Z. Y.; Yu, S. Y.; Zhang, R. B.; Wang, X.; Xu, H.; Wen, X.; Xi, Z. Discovery of *N*-phenyl-aminomethylthioacetylpyrimidine-2,4-diones as protoporphyrinogen IX oxidase inhibitors through a reaction intermediate derivation approach. *J. Agric. Food Chem.* **2021**, *69*, 4081–4092.

(36) Wang, D. W.; Zhang, R. B.; Yu, S. Y.; Liang, L.; Ismail, I.; Li, Y. H.; Xu, H.; Wen, X.; Xi, Z. Discovery of novel *N*-isoxazolinyphenyl-triazinones as promising protoporphyrinogen IX oxidase inhibitors. *J. Agric. Food Chem.* **2019**, *67*, 12382–12392.

(37) Zhou, Y.; Yu, Y.; Huang, Q.; Zheng, H.; Zhan, R.; Chen, L.; Meng, X. Simultaneous determination of 26 pesticide residues in traditional Chinese medicinal leeches by modified QuEChERS coupled with HPLC-MS/MS. *ACS Omega* **2023**, *8*, 12404–12410.